Published in final edited form as:
Female Pelvic Med Reconstr Surg. 2012 ; 18(3): 148–152. doi:10.1097/SPV.0b013e31824b76bd.

Estrogen Affects the Glycosaminoglycan Layer of the Murine Bladder

Mallika Anand, MD, **Caihong Wang, PhD**, **Jacob French**, **Megan Isaacson-Schmid, BS**, **L. Lewis Wall, MD, PhD**, and **Indira U. Mysorekar, PhD**
Department of Obstetrics and Gynecology, Washington University School of Medicine, St Louis, MO

Abstract

Objectives—Urinary tract infections (UTIs), commonly caused by uropathogenic *Escherichia coli* (UPEC), confer significant morbidity among postmenopausal women. Glycosaminoglycans (GAGs) comprise the first line of defense at the bladder's luminal surface. Our objective was to use a murine model of menopause to determine whether estrogen status affects the GAG layer in response to UPEC infection.

Methods—Adult female mice underwent sham surgery (SHAM, n = 18) or oophorectomy (OVX, n = 66) to establish a murine model of menopause. A subset of oophorectomized mice underwent hormone therapy (HT, n = 33) with 17β-estradiol. Mice were inoculated with UPEC and killed at various time points; bladders were collected and GAG layer thickness was assessed in multiple bladder sections. Sixteen measurements were made per bladder. A repeated-measures 2-way analysis of variance was performed to determine the effect of time after infection and hormonal condition on GAG thickness. We also investigated the molecular underpinnings of GAG biosynthesis in response to alterations in estrogen status and infection.

Results—We did not observe significant difference of GAG thickness among the 3 hormonal conditions; however, the time course of GAG thickness was significantly different ($P<0.05$). The OVX mice demonstrated significantly greater thickness at 72 hours after infection ($P = 0.0001$), and this effect was shifted earlier (24 hours after infection) on the addition of HT ($P = 0.001$). At 2 to 4 weeks after infection, GAG thickness among all cohorts was not significantly different from baseline. In addition, quantitative reverse transcription–polymerase chain reaction analysis revealed that GAG biosynthesis is altered by estrogen status at basal level and on infection.

Conclusions—The GAG layer is dynamically altered during the course of UTI. Our data show that HT positively regulates GAG layer thickness over time, as well as the composition of the GAGs. In addition, the GAG sulfation status can be influenced by estrogen levels in response to UPEC infection. The protective effects of the GAG layer in UTI may represent pharmacologic targets for the treatment and prevention of post-menopausal UTI.

Keywords

murine bladder; urinary tract infection; glycosaminoglycan; estrogen; hormone therapy

Reprints: Indira U. Mysorekar, PhD, Department of OB/GYN, 425 S Euclid Ave, Campus Box 8064, St Louis, MO 63110., mysorekari@wudosis.wustl.edu.
Drs Mallika Anand and Caihong Wang contributed equally to the work.

The authors declare that they have nothing to disclose.

Urinary tract infections (UTIs) confer significant morbidity among postmenopausal women. The overall annual incidence of UTIs in postmenopausal women is 7%.[1] Women aged 55 years and older have a 53% chance of experiencing recurrent UTI, and uropathogenic *Escherichia coli* (UPEC) are implicated in approximately 78% of recurrences.[2] Estrogen status—specifically, decreased estrogen as during menopause—is a significant risk factor for UTI. The lack of estrogen has been associated with urogenital tract changes that predispose to colonization with UPEC.[3,4] Uropathogenic *E. coli* infection follows a multistep pathway of infection, including adhesion, invasion, replication, and persistence.[5–7]

The first line of defense against infection at the bladder's luminal surface consists of the extracellular glycosaminoglycan (GAG) layer of the bladder.[8,9] Glycosaminoglycans are negatively charged polysaccharide chains that are found in multiple cellular locations and are involved in numerous cellular functions including cell-matrix interactions and activation of chemokines, enzymes, and growth factors. Some of the commonly known GAGs include hyaluronic acid, chondroitin sulfate, and heparan sulfate. In the bladder, the luminal surface contains a greater concentration of sulfated (negatively charged) GAGs than the intracellular and interstitial locations.[10] The thickness of the luminal surface of the GAG layer is thought to be approximately 10 to 20 μM on average.[11–13] Glycosaminoglycan sequences are not directly encoded by genes but are assembled in the Golgi apparatus by enzymes encoded by more than 40 genes.[14] Glycosaminoglycans may present unique sulfation patterns, chain lengths, and fine structures that permit them to rapidly adapt to a variety of environmental factors.[14–21]

Our objectives were to determine (1) whether estrogen status affects the GAG layer of the bladder at the basal level and in response to UPEC infection and (2) whether administration of exogenous estrogen would alter the GAG layer's regeneration after infection. We hypothesized that a hypoestrogenic state would impair the protective GAG layer and that estrogen replacement would restore this layer. Furthermore, we hypothesized that a subset of enzymes involved in GAG biosynthesis may be under estrogenic regulatory control.

MATERIALS AND METHODS

Murine Model of Surgical Menopause and Hormone Therapy

Approval for this study was obtained from the Institutional Animal Care and Use Committee. We established a murine model of menopause in which 7- to 8-week-old adult female C57BL6/J mice were anesthetized and underwent sham surgery (SHAM, n = 18) or oophorectomy (OVX, n = 66). The mice underwent a 2-week recovery period. A subset of oophorectomized mice underwent hormone therapy (HT, n = 33) with subcutaneous implantation of time-release pellets containing supratherapeutically dosed 0.01 mg of β-estradiol (Innovative Research of America, Sarasota, Fla).

Mouse Inoculations

Mice were anesthetized and inoculated with UTI89, a uropathogenic strain of *E. coli*. Inoculation was performed via transurethral catheterization with 50 μL of bacterial suspension (10^7 CFU/mL) of UTI89 in phosphate-buffered saline. The mice were killed at various time points after infection. For the uninfected time point (0 hours), 3 mice from each category (SHAM, OVX, and HT) were killed. At each of the remaining time points (6 hours, 24 hours, 72 hours, 2 weeks, and 4 weeks), 3 SHAM, 6 OVX, and 6 HT mice were killed. The bladders were collected, embedded in paraffin, and sectioned (Fig. 1).

Histochemical Analysis

Bladders were stained with Alcian blue, a positively charged histologic stain. Alcian blue was selected for its strong positive charge and thereby high avidity for the negatively charged, sulfated GAGs present at the luminal surface of the bladder[22] (Fig. 2). The thickness of the GAG layer was assessed in multiple bladder sections. Sections were visualized using a light microscope, a Nikon Eclipse E800 (Nikon, Tokyo, Japan) with an Olympus DP71 camera (Olympus, Tokyo, Japan). Images were captured and measurements made at 100× using ImageJ (National Institutes of Health, Bethesda, Md). Sixteen measurements were made per bladder.

Statistical Analysis

The measurements were collectively analyzed using a repeated-measures 2-way analysis of variance to determine the effect of time after infection and hormonal condition on GAG thickness on SHAM and OVX mice, including the subset of mice that underwent exogenous β-estradiol administration. Statistical analyses were made using SPSS 16.0 for Mac (IBM, Chicago, Ill).

Quantitative Real-time Polymerase Chain Reaction Analysis

We analyzed the expression of enzymes involved in GAG synthesis using real-time quantitative polymerase chain reaction (PCR) of RNA samples isolated and pooled from bladders of SHAM and OVX mice (n = 5 mice per sample). Samples were taken 6 hours after infection and from phosphate buffered saline controls at the same time points. RNA was isolated from the bladder using TRIzol (Invitrogen Life Technologies, Grand Island, NY), treated with DNase I (Ambion, Austin, Tex) to remove contaminating DNA, and complementary DNAs were synthesized from 2 μg of total RNA pooled from 5 bladders of each group using SuperScript II RNase H reverse transcriptase (Invitrogen Life Technologies). The expression of targets was detected by real-time PCR using the ABI Prism 7700 sequence detection system and SYBR Green PCR MasterMix (Applied Biosystems, Carlsbad, Calif). The primers used for detection of the targets are listed in Table 1. The expression of each target was measured in triplicate. Relative quantification of target expression was determined using the comparative C_T method with 18S expression as a control, as described in the ABI Prism 7700 Sequence Detection System User Bulletin.

RESULTS

Estrogen Status Alters the Thickness of the GAG Layers

The GAG thickness among the 3 hormonal conditions did not significantly differ at baseline; mean thicknesses were as follows: SHAM, 26.2 μm; OVX, 29.1 μm; and HT, 25.0 μm. Excitingly, however, we found that the time course of the GAG thickness was significantly different across hormonal conditions ($P = 0.034$). At 24 hours after infection, GAG thickness in estrogen-treated mice (29.3 μm) was significantly greater than that in SHAM (19.5 μm) and OVX (23.4 μm) mice ($P = 0.001$). At 72 hours after infection, GAG thickness in OVX mice (36.1 μm) was significantly greater than that in SHAM (21.5 μm) and estrogen-treated (27.2 μm) mice ($P = 0.0001$). By 4 weeks after infection, GAG thickness across all conditions had returned to levels not significantly different from baseline (SHAM, 26.0 μm; OVX, 28.7 μm; HT, 26.6 μm). Therefore, although the overall thickness of the GAG layer among the 3 hormonal conditions did not differ at baseline, the dynamic response of the GAG layer over the time course of infection changed depending on estrogen status (Fig. 3).

Loss of Estrogen Signaling Alters the Expression of Enzymes Involved in GAG Biosynthesis

To further examine whether the composition of the GAG layer is altered by estrogen status at baseline and on infection, we looked at the messenger RNA levels of enzymes involved in GAG biosynthesis by quantitative PCR. Among 23 enzymes tested, glucuronosyltransferase (Gluc), which adds GlcA residue to GAG chains, was highly modulated by estrogen level. At baseline, all 3 isoforms of Gluc were upregulated in OVX mice, with a fold change relative to SHAM mice of 10.7, 6.5, and 3.1 for Gluc1, Gluc2, and Gluc3, respectively (Fig. 4A). However, their up-regulation in OVX mice was slower on infection compared with SHAM mice, SHAM mice showed a rapid and robust up-regulation of these enzymes at 6 hours after infection, with a fold change of 23.7, 47.3, and 52.3 for Gluc1, Gluc2, and Gluc3, respectively (Fig. 4B). Interestingly, HA synthase (HAS), which synthesizes hyaluronan, a free GAG component, showed a similar response to estrogen level with Gluc before and after infection. We found that all 3 isoforms of HAS were upregulated before infection (Fig. 4A), and their up-regulation was slower on infection compared with SHAM mice (Fig. 4B). We also found that sulfation enzymes—especially Hs6ST1—were regulated by estrogen level in response to UPEC infection, with a greater-than-2-fold up-regulation relative to SHAM mice at 6 hours after infection (Fig. 4B).

DISCUSSION

Our original hypothesis was that the GAG layer would be altered in OVX mice. However, we did not observe a significant difference in the thickness of the GAG layer between SHAM and OVX mice before infection. Rather, the expression profile of GAG biosynthesis enzymes were differentially regulated by estrogen status, which suggests that it is the composition, rather than the amount, of the GAG layer that is regulated by estrogen status at the basal level. However, the dynamic response of the GAG layer to UPEC infection was affected by estrogen status. Our data show that estrogen status influences the time course of change in GAG thickness. Estrogen therapy leads to an earlier increase in GAG thickness, whereas OVX without estrogen therapy and SHAM-operated mice demonstrated a delayed increase in GAG thickness. Exactly how this shift in GAG increase impacts infection remains unclear. Previous studies have shown that estrogen regulates proinflammatory cytokines such as IL-6,[23–25] which in turn regulate the expression of genes involved in the production of GAG components (including heparan sulfate D-glucosaminyl 3-*O*-sulfotransferase and hyaluronan synthase).[26,27] The dynamic response of the GAG layer to UPEC infection might reflect the dynamic response of proinflammatory cytokines affected by estrogen in response to infection.

The quantitative PCR analysis of GAG synthetic enzymes suggests that the level of estrogen does not affect the initiation of the polysaccharide chain, but instead affects the elongation and sulfation of the polysaccharide chain. Accordingly, the initiation of the polysaccharide chain by, for example, addition of the xylose unit to the protein bone is not affected by estrogen level. We have previously shown that levels of heparan sulfate D-glucosaminyl-3-*O*-sulfotransferase were increased directly on UPEC infection.[28] Here, we show that the levels of heparan sulfate 6-*O*-sulfotransferase are also modulated by estrogen levels on infection. We previously demonstrated that the expression of HAS was upregulated in response to UPEC infection in wild-type mice.[28] Here, we observed the expression of hyaluronic acid synthetase was increased at the basal level and quickly downregulated on UPEC infection in OVX mice compared with SHAM mice. In contrast to the other GAG families, HA is most likely found in vivo as a free GAG. Thus, our data demonstrate a broad role of estrogen in the regulation of GAG components in response to UPEC infection, suggesting that estrogen level not only affects the GAG layer associated with the urothelial

surface but also affects the free GAGs, which has significant implications for wound repair after infection.

Together, our data show that not only the dynamic change of GAG layer thickness but also the composition of the GAGs and its sulfation status can be affected by level of estrogen, which in turn affects the urothelial barrier and its susceptibility to environmental insult such as UPEC infection. Further studies are required to determine the exact links between hormonal condition, dynamic GAG thickness changes, GAG composition, and clearance of UPEC from the bladder. The GAG layer may represent potential pharmacologic targets for the treatment and prevention of postmenopausal UTI.

Acknowledgments

This study was supported by a grant from the National Institute of Diabetes and Digestive and Kidney (K99/R00 080643 to I.U.M.) and by a research grant from the Center for Women's Infectious Disease Research to C.W.

References

1. Jackson SL, Boyko EJ, Scholes D, et al. Predictors of urinary tract infection after menopause: a prospective study. Am J Med. 2004; 117:903–911. [PubMed: 15629728]
2. Ikäheimo R, Siitonen A, Heiskanen T, et al. Recurrence of urinary tract infection in a primary care setting: analysis of a 1-year follow-up of 179 women. Clin Infect Dis. 1996; 22:91–99. [PubMed: 8824972]
3. Stamm WE, Raz R. Factors contributing to susceptibility of postmenopausal women to recurrent urinary tract infections. Clin Infect Dis. 1999; 28:723–725. [PubMed: 10825026]
4. Dielubanza EJ, Schaeffer AJ. Urinary tract infections in women. Med Clin North Am. 2011; 95:27–41. [PubMed: 21095409]
5. Rosen DA, Hooton TM, Stamm WE, et al. Detection of intracellular bacterial communities in human urinary tract infection. PLoS Med. 2007; 4:e329. [PubMed: 18092884]
6. Mysorekar IU, Hultgren SJ. Mechanisms of uropathogenic *Escherichia coli* persistence and eradication from the urinary tract. Proc Natl Acad Sci U S A. 2006; 103:14170–14175. [PubMed: 16968784]
7. Justice SS, Hung C, Theriot JA, et al. Differentiation and developmental pathways of uropathogenic *Escherichia coli* in urinary tract pathogenesis. Proc Natl Acad Sci U S A. 2004; 101:1333–1338. [PubMed: 14739341]
8. Parsons CL, Stauffer C, Schmidt JD. Bladder-surface glycosaminoglycans: an efficient mechanism of environmental adaptation. Science. 1980; 208:605–607. [PubMed: 6154316]
9. Parsons CL, Stauffer CW, Schmidt JD. Reversible inactivation of bladder surface glycosaminoglycan antibacterial activity by protamine sulfate. Infect Immun. 1988; 56:1341–1343. [PubMed: 3281908]
10. Hurst RE, Rhodes SW, Adamson PB, et al. Functional and structural characteristics of the glycosaminoglycans of the bladder luminal surface. J Urol. 1987; 138:433–437. [PubMed: 3599272]
11. Nickel JC, Emerson L, Cornish J. The bladder mucus (glycosaminoglycan) layer in interstitial cystitis. J Urol. 1993; 149:716–718. [PubMed: 8455229]
12. Nickel JC, Egerdie B, Downey J, et al. A real-life multicentre clinical practice study to evaluate the efficacy and safety of intravesical chondroitin sulphate for the treatment of interstitial cystitis. BJU Int. 2009; 103:56–60. [PubMed: 18778342]
13. Nickel JC, Cornish J. Ultrastructural study of an antibody-stabilized bladder surface: a new perspective on the elusive glycosaminoglycan layer. World J Urol. 1994; 12:11–14. [PubMed: 8012410]
14. McDowell LM, Frazier BA, Studelska DR, et al. Inhibition or activation of Apert syndrome FGFR2 (S252W) signaling by specific glycosaminoglycans. J Biol Chem. 2006; 281:6924–6930. [PubMed: 16373332]

15. Esko, JD.; Kimata, K.; Lindahl, U. Proteoglycans and Sulfated Glycosaminoglycans. In: Varki, A.; Cummings, RD.; Esko, JD., et al., editors. Essentials of Glycobiology. 2. Cold Spring Harbor, NY: Cold Spring Harbor Laboratory Press; 2009.
16. David-Raoudi M, Deschrevel B, Leclercq S, et al. Chondroitin sulfate increases hyaluronan production by human synoviocytes through differential regulation of hyaluronan synthases: role of p38 and Akt. Arthritis Rheum. 2009; 60:760–770. [PubMed: 19248106]
17. DeAngelis PL. Molecular directionality of polysaccharide polymerization by the *Pasteurella multocida* hyaluronan synthase. J Biol Chem. 1999; 274:26557–26562. [PubMed: 10473619]
18. Itano N, Kimata K. Mammalian hyaluronan synthases. IUBMB Life. 2002; 54:195–199. [PubMed: 12512858]
19. Kusche-Gullberg M, Kjellen L. Sulfotransferases in glycosaminoglycan biosynthesis. Curr Opin Struct Biol. 2003; 13:605–611. [PubMed: 14568616]
20. Silbert JE, Sugumaran G. Biosynthesis of chondroitin/dermatan sulfate. IUBMB Life. 2002; 54:177–186. [PubMed: 12512856]
21. Kawashima H, Atarashi K, Hirose M, et al. Oversulfated chondroitin/ dermatan sulfates containing GlcAbeta1/IdoAalpha1–3GalNAc (4,6-*O*-disulfate) interact with L- and P-selectin and chemokines. J Biol Chem. 2002; 277:12921–12930. [PubMed: 11821431]
22. Scott JE. Alcian blue. Now you see it, now you don't. Eur J Oral Sci. 1996; 104:2–9. [PubMed: 8653492]
23. Boyce BF, Xing L, Franzoso G, et al. Required and nonessential functions of nuclear factor-kappa B in bone cells. Bone. 1999; 25:137–139. [PubMed: 10423039]
24. Galien R, Garcia T. Estrogen receptor impairs interleukin-6 expression by preventing protein binding on the NF-kappaB site. Nucleic Acids Res. 1997; 25:2424–2429. [PubMed: 9171095]
25. Pfeilschifter J, Koditz R, Pfohl M, et al. Changes in proinflammatory cytokine activity after menopause. Endocr Rev. 2002; 23:90–119. [PubMed: 11844745]
26. Wood MW, Breitschwerdt EB, Gookin JL. Autocrine effects of interleukin-6 mediate acute-phase proinflammatory and tissue-reparative transcriptional responses of canine bladder mucosa. Infect Immun. 2011; 79:708–715. [PubMed: 21115724]
27. Chen WY, Abatangelo G. Functions of hyaluronan in wound repair. Wound Repair Regen. 1999; 7:79–89. [PubMed: 10231509]
28. Mysorekar IU, Mulvey MA, Hultgren SJ, et al. Molecular regulation of urothelial renewal and host defenses during infection with uropathogenic *Escherichia coli*. J Biol Chem. 2002; 277:7412–7419. [PubMed: 11744708]

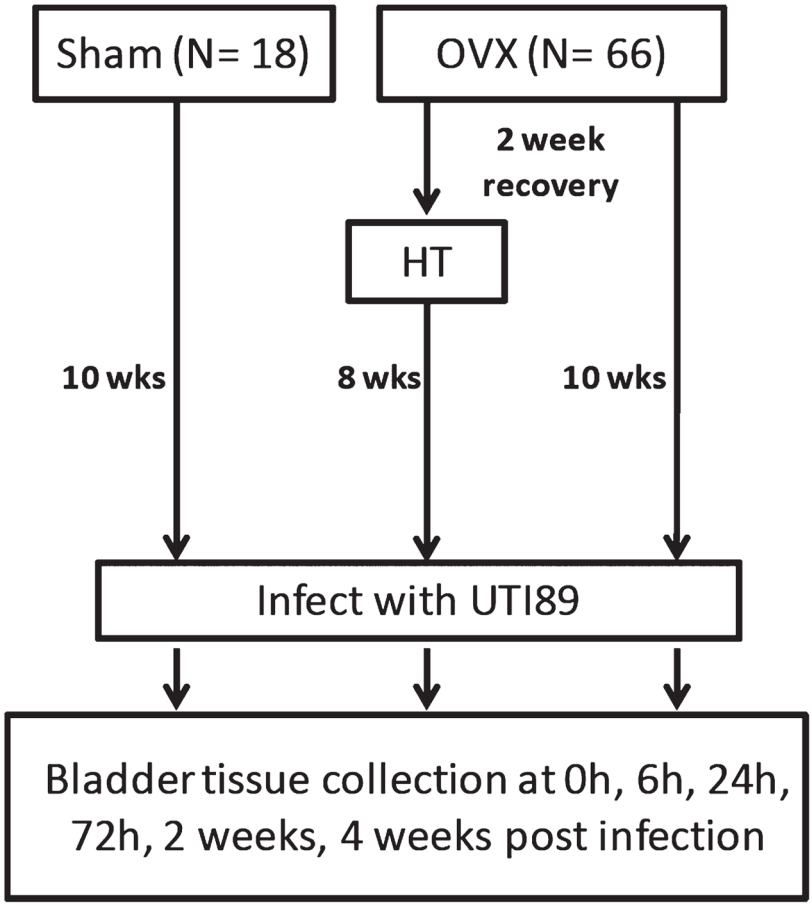

FIGURE 1.
Murine model of menopause.

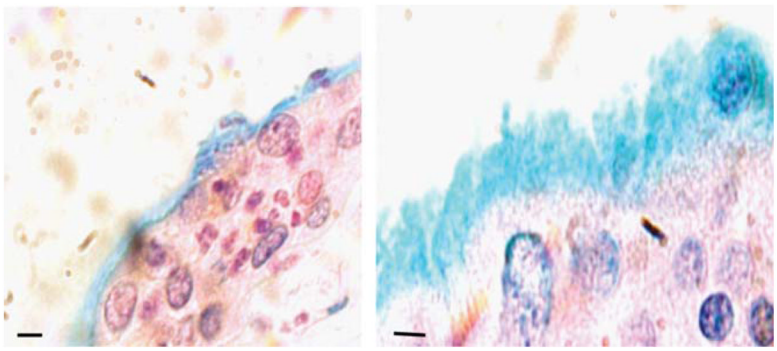

FIGURE 2.
Representative photomicrograph of Alcian blue staining in the bladder. Bar, 5 μm.

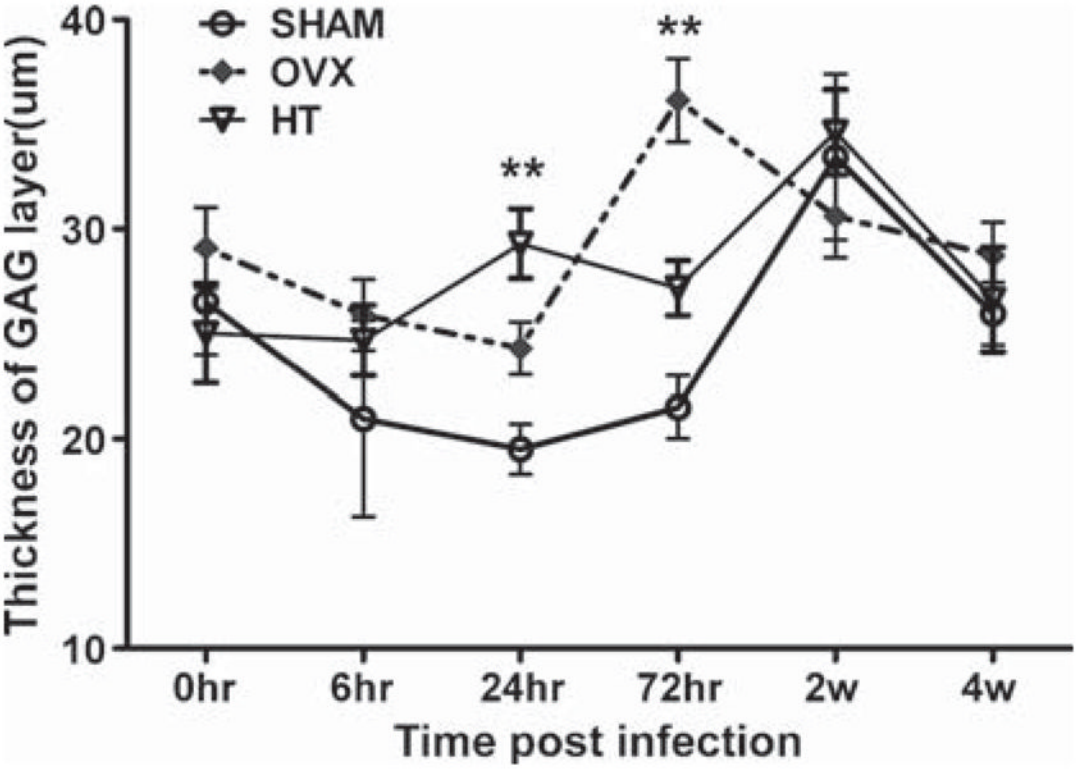

FIGURE 3.
Time course of GAG thickness is altered by hormonal condition.

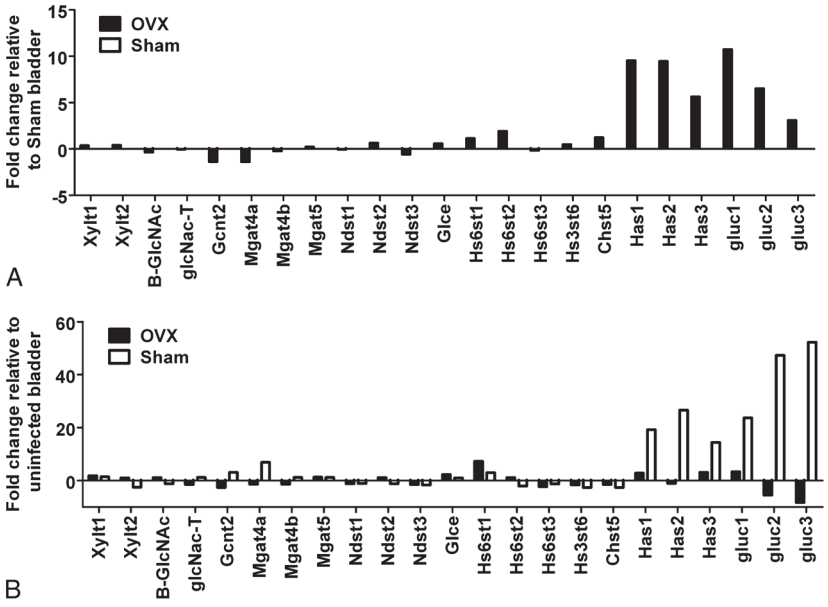

FIGURE 4.

Enzymes for GAG biosynthesis are regulated by estrogen status before and after UPEC infection.

TABLE 1

Primer List for GAG Biosynthesis Enzymes

Gene Name	Gene ID	5′ Primer	3′ Primer
Xylt1 xylosyltransferase 1	233781	TCCACAACCAAGTCCACTGAT	GCGAAGTTGCTGTTATCCACATT
Xylt1 xylosyltransferase 2	217119	GTGCGGGCAGTAACCAGTC	CAATCTCACACTTCGGAGTGAA
βGlcNAc β 1,4- galactosyltransferase II (β*GlcNAc*)	53418	TGCCTGCTGCACTTCCTTG	CAGGGCGGAATGACTGGAG
Galactosylgalactosylxylosylprotein 3-β-glucuronosyltransferase 1 (*Gluc1*)	76898	ACCATCCATGTGGTGACGC	CCACTAGCCAGTGAAGGTTGG
Galactosylgalactosylxylosylprotein 3-β-glucuronosyltransferase 2 (*Gluc2*)	280645	ACAGAGAAGGTCAATCTAGCCA	ACCTCAATGTTCACTGTGTCCA
Galactosylgalactosylxylosylprotein 3-β-glucuronosyltransferase 3 (*Gluc3*)	72727	CATTACCCCCACCTACGCC	CCCTAAGCCGTTGAGCCTT
α-1,3-mannosyl-glycoprotein 2-β-*N*-acetylglucosaminyltransferase (*glcNAc-T I*)	17308	TTGTGCTTTGGGGTGCTATCA	CCACAGTGGGAACTCTCCA
Glucosaminyl (*N*-acetyl) transferase 2, I-branching enzyme (*Gcnt2*)	14538	TCAGCCTATCTCTCATTGCTGC	CGCTGTCCGCTGTATAAAAACT
Mannoside acetylglucosaminyltransferase 4, isoenzyme A (*Mgat4a*)	269181	ATGAGGCTCCGAAATGGAACT	CCACTCGAAGACGCTCTTTTAG
Mannoside acetylglucosaminyltransferase 4, isoenzyme B (*Mgat4b*)	103534	GAGGGCAGTATCCGAGAGG	CGAGACGTTCCACGGCTTC
Mgat5 mannoside acetylglucosaminyltransferase 5	107895	CACTGCGAGGGGAAAATCAAG	CCACTCCATAGTCTGCGTAGC
N-deacetylase/*N*-sulfotransferase (heparan glucosaminyl) 1 (*Ndst1*)	15531	CTTCTGCCTGTTCAGCGTTTT	CAGTGGGTCTGTTCGGGAA
N-deacetylase/*N*-sulfotransferase (heparan glucosaminyl) 2 (*Ndst2*)	17423	CTGCTGATTGGTTTCAGTCTTGT	CCACTGCTACTACAGTCTCCC
N-deacetylase/*N*-sulfotransferase (heparan glucosaminyl) 3 (*Ndst3*)	83398	TGCTTGCCACCTTTTGTATGG	AGCATCGGAAATCATTGTCCTC
Glucuronyl C5-epimerase (*Glce*)	93683	GCAGCTCGGGTCAACTATAAG	TCCATCCACTCTGAATCCACT
Heparan sulfate 6-*O*-sulfotransferase 1 (*Hs6st1*)	50785	CGGACCCACATTACGAGAAAA	GATTGGGCCGATAGCAGGTG
Heparan sulfate 6-*O*-sulfotransferase 2 (*Hs6st2*)	50786	TTCTCCAAGATTTTCGGTCCCT	ACCGCAAATAGGAAGAGCATC
Heparan sulfate 6-*O*-sulfotransferase 3 (*Hs6st3*)	50787	GATGAAAGGTTCAACAAGTGGC	CGAAGTTGGTGCATGAGCTG
Heparan sulfate (glucosamine) 3-*O*-sulfotransferase 6 (*Hs3st6*)	328779	TTCTTCGACAGGTGCTATGATCG	CCAGGGTCCGTGGCATTAG
Carbohydrate (*N*-acetylglucosamine 6-*O*) sulfotransferase 5 (*Chst5*)	56773	GTGCTGGTACTGTCCTCGTG	CGCATAGGAACACTGAGCGG
Mus musculus hyaluronan synthase1 (*Has1*)	15116	GGCGAGCACTCACGATCATC	AGGAGTCCATAGCGATCTGAAG
Mus musculus hyaluronan synthase 2 (*Has2*)	15117	TGTGAGAGGTTTCTATGTGTCCT	ACCGTACAGTCCAAATGAGAAGT
Mus musculus hyaluronan synthase 3 (*Has3*)	15118	CCTGGAGCACCGTCGAATG	CCTTGAGGTTTGGAAAGGCAA